RADIAL MATCHING IN FOUR-ROD-RFQS

P. Junior, H. Deitinghoff, M. Malouschek

Institut für Angewandte Physik der Johann-Wolfgang-Goethe-Universität,
Postfach 111 932, D-6000 Frankfurt am Main 1, FRG

Abstract

Particle acceleration in RFQ linacs usually starts with a radial matching section. In case of the "four-rod" configuration 4 fingers jut out of the rods, in this way matching the dc ion beam to the rotating acceptance of the RFQ channel or the output beam to further devices. The paper reports typical behaviour of both transverse and longitudinal particle motion as effected by field harmonics, which are inherent with such fingers.

Taking up suggestions as noted in [1] we expand the potential function according to equ. (1)

$$\Phi(r,\vartheta,z,t) = \frac{AV}{2} \cos\omega t \left[\cos2\vartheta F_1(r,z) + \cos6\vartheta F_2(r,z) \right] \quad (1)$$

$$F_1(r,z) = \sum_{J=1}^{3} C_i I_2(ikr) \cos ikz$$

$$F_2(r,z) = \sum_{J=1}^{3} D_i I_6(ikr) \cos ikz$$

$$i = 2J - 1$$

Fig. 1 explains the periodic sequence of the corresponding electrodes. The section, where this potential guides the beam, is accentuated. From the junction at $z = 0$ onwards the RFQ is assumed to consist of plain electrodes, the radial matcher reaches from the diaphragma at $z = -L$ to $z = 0$. This distance amounts to $N\beta\lambda/2$ cells defining a wave number

$$k = \frac{\pi}{2L} = \frac{\Omega}{v}/2N$$

Expansion coefficients should be chosen in that way that the field gradient has a suitable slope, linear growth is accomplished by $C_i = 1/i^4$, electrode radius and aperture agree with each other, when we decide for $D_i = 0.32\, C_i$. This fixation is held throughout in the paper. Fig. 2 shows the corresponding electrode.

The factor A in equ. (1) stands for the regular transition of the potential (1) to the one, which starts with plain electrodes at $z = 0$ giving equ. (2)

$$A = \sum_{J=1}^{3} C_i I_2(ikr) + D_i I_6(ikr) \quad (2)$$

$$i = 2J - 1$$

Fig. 3 demonstrates the intersecting curve of the electrode within the x-z plane and the almost linear growth of the field gradient. Particle motion follows equations (3a), (4)

$$\frac{d^2r}{dt^2} = -\frac{eAVk}{2m} \cos\omega t \left[\cos2\vartheta G_1(r,z) + \cos6\vartheta G_2(r,z) \right] \quad (3a)$$

$$G_1 = \sum_{J=1}^{3} iC_i \left[I_1(ikr) - \frac{2}{ikr} I_2(ikr) \right] \cos ikz$$

$$G_2 = \sum_{J=1}^{3} iD_i \left[I_5(ikr) - \frac{6}{ikr} I_6(ikr) \right] \cos ikz$$

$$i = 2J - 1$$

$$\frac{d^2u}{dt^2} = +\frac{eAVk}{2m} \cos\omega t \left[\cos2\vartheta H_1(r,z) + \cos6\vartheta H_2(r,z) \right] \quad (4)$$

$$H_1 = \sum_{J=1}^{3} iC_i I_2(ikr) \sin ikz$$

$$H_2 = \sum_{J=1}^{3} iD_i I_6(ikr) \sin ikz$$

$$i = 2J - 1$$

for the longitudinal motion (4) u means the longitudinal deviation from $z_S = vt - L$, i.e. $u = z - z_S$. When we expand the Besselfunctions I_1 and I_2, neglect I_5 and I_6 and cut off all higher exponentials than 2, equation (3a) becomes linear

$$\frac{d^2r}{dt^2} = -\frac{eE'(z)}{m} \; r \; \cos2\vartheta \; \cos\omega t \qquad (3b)$$

$$E'(z) = \frac{AVk^2}{8} \sum_{J=1}^{3} i^2C_i \; \cos ikz$$

$$i = 2J - 1$$

Solving the corresponding envelope equ. backward from z = 0 to z = - L, where at z = 0 the matched beam with respect to the plain RFQ is initially taken, the x-z and y-z envelopes are illustrated in fig. 3 also. At z = - L both emittances $x\frac{dx}{dt}$ and $y\frac{dy}{dt}$ with area $\pi\varepsilon$ overlap only to a certain extend. Contrarily to [1] we define the mismatch factor Mism with the overlap area πF by

$$Mism = 1 - \frac{F}{\varepsilon} \qquad (5)$$

When the overlap is perfect F = ε and Mism = 0 when it is faulty Mism → 1. So the intersecting area F = (1 - Mism) · ε stands for the total channel accep tance. Fig. 4 illustrates this, and it is easily seen that it generally differs from the mismatch factor as defined in [1]. In order to check up our above state ment concerning the channel acceptance F with re spect to nonlinear effects caused by the external field of equ. (1), F is again transported from z = - L to z = 0; however, for this procedure the general equa tions of motion (3a) and (4) are solved. From fig. 5 we learn that the beam is not effected by those non linearities, energy spread due to longitudinal field components remains moderate. Table I summarizes our calculations. For the 20 mA evaluations the well known KV expressions[2] were inserted in the right hand side of equation (3b). Table I hints the N = 4 $\beta\lambda/2$ configuration, here maximum energy spread is small at a still moderate mismatch factor. Simula tions using the PARMTEQ code accentuate the satis fying performance of this matcher. All calculations refer to the RFQ design with $\omega = 2\pi \cdot 27$ MHz, V = 180 kV, R = 6.8 mm, Xe_{131}^{1+}, input energy 39.3 MeV. Computations have been carried out at the HRZ of the university of Frankfurt.

Table 1

N	J [mA]	ε [m²/s]	Mism [%]	δW/W [%]	L [cm]
4	0	0.449 · 10³	12.3	0.062	4.9
	20	0.432 · 10³	12.5		4.9
6	0	0.449 · 10³	12.4	0.012	7.36
	20	0.432 · 10³	12.6		7.36
8	0	0.449 · 10³	12.5	0.062	9.8
	20	0.432 · 10³	12.7		9.8
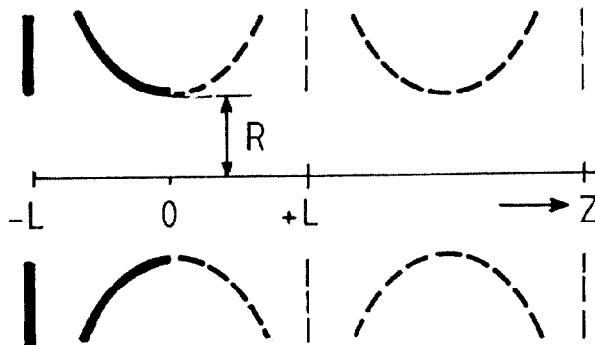
Fig. 1. Periodic electrode sequence
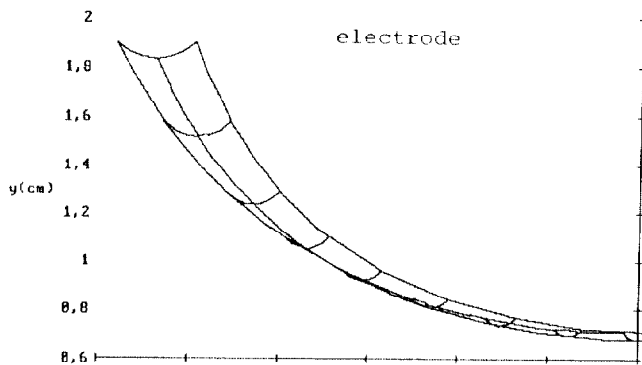
Fig. 2 Electrode finger example

References

[1] K.R. Crandall, Proc. 1984 Lin. Acc. Conf., GSI-84-11 p. 109

[2] I.M. Kapchinskiy, V.V. Vladimirksiy, Proc. Intern. Conf. on High Energy Acc., CERN 1959, p. 274
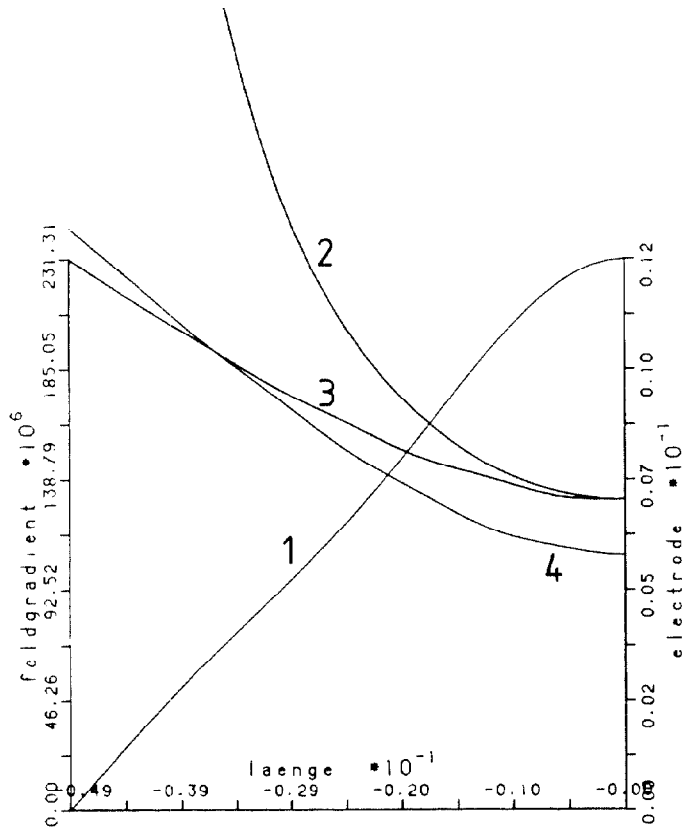
Fig. 3 1. Fieldgradient $E'(z)$
   2. Electrode intersection in x-z-plane
   3. Beam envelope x(z) in x-z-plane
   4. Beam envelope y(z) in y-z-plane

Fig. 5 Phase space $x - \frac{dx}{dt}$
   1. Acceptance at z = - L
   2. Transported acceptance at z = 0
   3. Acceptance of RFQ at z = 0
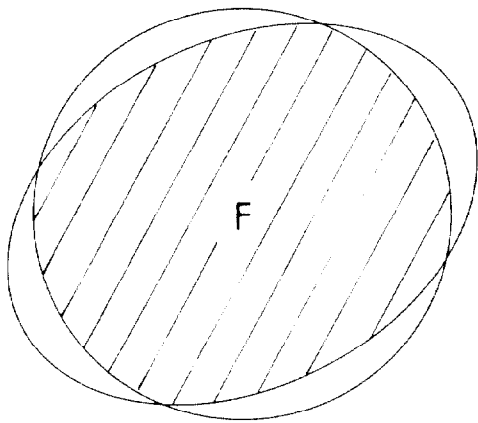
Fig. 4 Channel acceptance F of equ. (5)